JPn Neuroscience

The Journal of Physiology

J Physiol 593.16 (2015) pp 3739–3755

Increased excitability of medium-sized dorsal root ganglion neurons by prolonged interleukin-1β exposure is K^+ channel dependent and reversible

Patrick L. Stemkowski[1], Myung-chul Noh[2], Yishen Chen[2] and Peter A. Smith[2]

[1] *Department of Physiology and Pharmacology, Hotchkiss Brain Institute, University of Calgary, Calgary, Canada, T2N 4N1*
[2] *Centre for Neuroscience and Department of Pharmacology, University of Alberta, Edmonton, Alberta, Canada, T6G 2H7*

Key points

- Neuropathic pain resulting from peripheral nerve injury is initiated and maintained by persistent ectopic activity in primary afferent neurons.
- Sciatic nerve injury increases the excitability of medium-sized dorsal root ganglion (DRG) neurons. Levels of the inflammatory cytokine interleukin 1β (IL-1β) increase and peak after 7 days.
- Five to six days of exposure of medium sized DRG neurons to 100 pM IL-1β promotes persistent increases in excitability which abate within 3–4 days of cytokine removal. This is associated with a profound attenuation of K^+ channel currents but only modest increases in function of cyclic nucleotide-sensitive hyperpolarization-activated channels (HCNs) and of voltage-gated Na^+ and Ca^{2+} channel currents.
- It is unlikely, therefore, that direct interaction of IL-1β with DRG neurons is capable of initiating an enduring phenotypic shift in their electrophysiological properties that follows sciatic nerve injury.
- The findings also underline the importance of K^+ channel modulation in the actions of inflammatory mediators on peripheral neurons.

Abstract Chronic constriction injury of rat sciatic nerve promotes signs of neuropathic pain. This is associated with an increase in the level of interleukin 1β (IL-1β) in primary afferents that peaks at 7 days. This initial cytokine exposure has been proposed to trigger an enduring alteration in neuronal phenotype that underlies chronic hyper-excitability in sensory nerves, which initiates and maintains chronic neuropathic pain. We have shown previously that 5–6 days of exposure of rat dorsal root ganglia (DRGs) to 100 pM IL-1β increases the excitability of medium-sized neurons. We have now found using whole-cell recording that this increased excitability reverts to control levels within 3–4 days of cytokine removal. The effects of IL-1β were dominated by changes in K^+ currents. Thus, the amplitudes of A-current, delayed rectifier and Ca^{2+}-sensitive K^+ currents were reduced by ~68%, ~64% and ~36%, respectively. Effects of IL-1β on other cation currents were modest by comparison. There was thus a slight decrease in availability of high voltage-activated Ca^{2+} channel current, a small increase in rates of activation of hyperpolarization-activated cyclic nucleotide-gated channel current (I_H), and a shift in the voltage dependence of activation of tetrodotoxin-sensitive sodium current (TTX-S I_{Na}) to more negative potentials. It is unlikely, therefore, that direct interaction of IL-1β with DRG neurons initiates an enduring phenotypic shift in their electrophysiological properties following sciatic nerve injury. Persistent increases in primary afferent excitability following nerve injury may instead depend on altered K^+ channel function and on the continued presence of slightly elevated levels IL-1β and other cytokines.

DOI: 10.1113/JP270905

(Received 8 May 2015; accepted after revision 17 June 2015; first published online 23 June 2015)
Corresponding author P. A. Smith: Department of Pharmacology, 9-75 Medical Sciences Building, University of Alberta, Edmonton, AB, Canada, T6G 2H7. Email: peter.a.smith@ualberta.ca

Abbreviations AP, action potential; BSA, bovine serum albumin; CCI, chronic constriction injury; DRG, dorsal root ganglion; DMEM, Dulbecco's modified Eagle's medium; DMEMHS, Dulbecco modified Eagle's medium with heat inactiavted serum; ERK, extracellular signal regulated kinase; HBSS, Hepes-buffered saline solution; HCN, hyperpolarization-activated cyclic nucleotide-gated (channels); HIV, human immunodeficiency virus; HVA-I_{Ba}, current carried by Ba^{2+} through high voltage activated Ca^{2+} channels; I_{Ba}, current carried by Ba^{2+} through Ca^{2+} channels; I_{Ca}, calcium channel current; I_H, current through HCN channels; I_K, K^+ channel current; I_{Na}, Na^+ channel current; IL-β, interleukin 1β; IB_4, isolectin B_4; NGF, nerve growth factor; PBS, phosphate buffered saline; RMP, resting membrane potential; TNF-α, tumour necrosis factor alpha; TTX-R I_{Na}, tetrodotoxin-resistant Na^+ channel current; TTX-S I_{Na}, tetrodotoxin-sensitive Na^+ channel current; V_{cmd}, command potential (in voltage clamp experiments); V_h, holding potential (in voltage clamp experiments).

Introduction

Pain is a vital physiological process that signals actual or potential tissue damage. By so doing, it protects from injury and secures the survival of the species. By contrast, injury to the somatosensory system can produce 'neuropathic' pain that lasts for months or years after any injury has healed (Treede *et al.* 2008; Costigan *et al.* 2009). This maladaptive 'disease of pain' has a 1.5–3% prevalence within the general population (Gilron *et al.* 2006) and can be associated with diabetic, post-herpetic or HIV-related neuropathies, fibromyalgia and osteoarthritis, and traumatic nerve, spinal cord or brain injury (including stroke) (Baron *et al.* 2010). Several lines of evidence implicate a transient, inflammatory response in the initiation of neuropathic pain (Watkins & Maier, 2002; Scholz & Woolf, 2007). This initial response is thought to produce slower genomic changes that lead, over a period of weeks or months, to a chronic neuropathic state.

Although acute exposure of dorsal root ganglion (DRG) neurons to pro-inflammatory cytokines such as interleukin 1β (IL-1β) is known to increase their excitability (Binshtok *et al.* 2008), little is known about the aftermath of cytokine exposure and how this may trigger enduring changes in neuronal excitability and/or phenotype as a result of altered expression of ion channels and/or their regulatory proteins (Stemkowski & Smith, 2012*b*).

Sciatic nerve chronic constriction injury (CCI) is one of several rodent models used to study the aetiology of neuropathic pain (Mosconi & Kruger, 1996; Kim *et al.* 1997). This has been reported to increase levels of IL-1β in sciatic nerve extracts (Nadeau *et al.* 2011). Since cytokine levels peak at 7 days (Nadeau *et al.* 2011), we recently examined the effect of 5–6 days of exposure of DRG neurons to IL-1β (100 pM). As is seen with acute application (Binshtok *et al.* 2008), we found that prolonged exposure to IL-1β increases the excitability of medium-diameter neurons and small isolectin B_4 (IB_4)-positive neurons, but large neurons and small IB_4 negative neurons were less affected (Stemkowski & Smith, 2012*a*). Because nocigenic ectopic activity in sensory nerves can persist for weeks, months or years after an initial insult (Govrin-Lippmann & Devor, 1978; Wall *et al.* 1979; Abdulla & Smith, 2001*a*; Pitcher & Henry, 2008; Devor *et al.* 2014; Vaso *et al.* 2014) and may play a major role in the maintenance of chronic pain (Sukhotinsky *et al.* 2004; Pitcher & Henry, 2008; Vaso *et al.* 2014), we asked whether this transient, 5–6 days of, exposure to IL-1β (Stemkowski & Smith, 2012*a*) can produce irreversible increases in sensory neuron excitability. If this were the case, it would implicate IL-1β as an insigator of a shift in the phenotype of sensory nerves that contributes to chronic neuropathic pain (Nitzan-Luques *et al.* 2011). We studied medium-sized DRG neurons as, in addition to there relative high sensitivity to IL-1β (Stemkowski & Smith, 2012*a*), their excitability, as well as that of their associated Aδ fibres, is increased following peripheral nerve injury (Kajander & Bennett, 1992; Abdulla & Smith, 2001*a*; Ma *et al.* 2003).

Changes in the properties of ion channels in medium-sized DRG neurons following various types of chronic nerve injury have been chracterised (Baccei & Kocsis, 2000; Abdulla & Smith, 2001*b*, 2002; Yao *et al.* 2003; Tan *et al.* 2006; Stemkowski & Smith, 2012*b*), but little is known of how these channels may be affected by IL-1β. Addressing this question represents a second objective of our study. Experiments were done in neuron-enriched cultures to minimize any indirect effects of IL-1β mediated via macrophages or glial cells. Preliminary reports of some of these findings have appeared (Stemkowski & Smith, 2010; Stemkowski *et al.* 2011).

Methods

Ethical approval

All experimental procedures were reviewed and approved by the University of Alberta Health Sciences Laboratory Animal Services Welfare Committee, and complied with the guidelines of the Canadian Council for Animal Care.

Primary cell cultures

Male Sprague–Dawley rats (18–20 days old) were killed with a high dose of 1.5 g kg^{-1} ethyl carbamate (urethane; I.P.; Sigma, St Louis, MO, USA). DRGs (14–21 per animal) were aseptically dissected from thoracic and lumbar spinal segments and collected in Dulbecco's modified Eagle's medium supplemented with 10% heat-inactivated horse serum (DMEMHS; both from Gibco, Grand Island, NY, USA). Ganglia were treated for 1.5 h at 34°C with 0.125% type IV collagenase (Worthington, Lakewood, NJ, USA), washed twice in Ca^{2+}/Ba^{2+}-free phosphate buffered saline (PBS), treated with 0.25% trypsin from bovine pancreas (Sigma) in PBS for 30 min, washed 3 times in DMEMHS and finally taken up in 2 ml of DMEMHS containing 80 μg ml^{-1} type IV DNAse (Sigma) and 100 μg ml^{-1} soybean trypsin inhibitor (Worthington). A single-cell suspension was then readily obtained by trituration of the enzymatically softened ganglia by six to eight passages through the tip of a 1 ml Eppendorf pipette. Neurons were plated the following day after neuronal cell enrichment.

Neuronal cell enrichment

Neuronal cell enrichment (Lindsay, 1988) was aimed at minimizing any effects of IL-1β mediated indirectly as a result of actions on mitotic (non-neuronal) cells that may be present in the cultures and the subsequent release of mediators, such as eicosanoids and growth factors. Non-neuronal cells were largely eliminated at the outset by the use of differential adhesion and treatment with anti-mitotic agents, followed by differential sedimentation procedures. More specifically, dissociated ganglia were plated (in DMEMHS supplemented with the anti-mitotic combination of cytosine 3-D-arabino-furanoside (Ara-C), uridine and 5-fluoro-2′-deoxyuridine (all from Sigma and all at 10 μM)) in two 50 mm culture dishes (preplates; Corning, NY, USA) previously coated with 3 μg ml^{-1} polyornithine (Sigma). After 15–20 h, the non-neuronal cells became firmly attached to the dish, while most of the neurons were only weakly adherent to the dish or to flattened non-neuronal cells. Then, by carefully removing the culture medium, most dead cells and axonal and myelin debris were discarded prior to selectively dislodging the attached neurons with a gentle stream of serum free defined medium (DMEM supplemented with 1/100 N-2 supplement and 1/100 penicillin–streptomycin–amphotericin B (all from Gibco)) delivered from a 1 ml Eppendorf pipette. The neurons from the two preplates were collected in a total of 12 ml of defined medium in a conical test tube. Further neuronal enrichment was achieved by centrifugation of the cell suspension at 28 g for 5 min, whereupon viable neurons are lightly pelleted, leaving myelin debris, dead cells and small non-neuronal cells in suspension. The supernatant was discarded and the cells were then re-suspended in 1 ml of defined medium. At 100 μl volumes, the cells were plated onto 35 mm tissue culture dishes (Nunc, Roskilde, Denmark) pre-coated with 3 μg ml^{-1} polyornithine (Sigma) and 2 μg ml^{-1} laminin (Sigma). Dishes were then filled with a serum-free defined medium at ∼2 ml per dish. Cells were maintained at 36.5°C, 95% air, 5% CO_2. Medium was exchanged every 72 h.

Treatment of DRG neurons

After 3 days in culture, dishes were divided into two treatment groups: 100 pM IL-1β (Peprotech, Rocky Hill, NJ, USA; prepared in 0.1% BSA (Sigma)) and control (0.1% BSA). Treatments were applied for the following 5–6 days, with defined medium exchanges every 72 h.

Two other groups were pretreated with 50 ng ml^{-1} nerve growth factor (NGF; Alomone Labs, Jerusalem, Israel; prepared in 0.1% BSA (Sigma) dissolved in Hepes-buffered saline solution (HBSS)) following the initial DRG isolation (Day 0). After 3 days in culture with NGF, dishes were divided into two groups, both of which received continued supplementation with 50 ng ml^{-1} NGF. One group of cultures received 100 pM IL-1β (Peprotech; prepared in 0.1% BSA (Sigma)), and the other served as control (0.1% BSA). Treatments were applied for the following 5–6 days, with defined medium (supplemented with 50 ng ml^{-1} NGF) exchanges every 72 h.

To examine recovery from IL-1β effects, cultures were exposed to cytokine for 5–6 days as described above and then maintained in culture without cytokine for a further 3–4 days prior to electrophysiological analysis. Control cultures were maintained for 10–12 days prior to study. These protocols are illustrated schematically in Fig. 1.

Subclassification of DRG neurons

Based on previously established criteria, DRG neurons were classified according to soma diameter as 'small' (<30 μm), 'medium' (30–40 μm), or 'large' (>40 μm) as measured with a calibrated micrometer fitted to the eye-piece of a Nikon TE300 inverted fluorescence microscope (Nikon, Toronto, ON, Canada). All recordings were made from neurons with medium-sized cell bodies, which are likely to represent a mixed population of nociceptive and non-nociceptive afferents (Aδ-fibres) (Harper & Lawson, 1985; Lawson, 2002).

Electrophysiology

Whole-cell recordings (at room temperature, 22°C) were made using an Axoclamp 2A amplifier (Axon Instruments, Foster City, CA, USA) in either bridge-balance

current-clamp mode or discontinuous single-electrode voltage-clamp mode as described previously (Abdulla & Smith, 2001*a*,*b*, 2002). With regard to voltage-clamp studies, low resistance patch electrodes (2–5 MΩ) permitted the use of high switching frequencies >30 kHz with high clamp gains (8–30 mV nA^{-1}). The effectiveness of the voltage-clamp was confirmed by examining recordings of the command voltage, and recordings from neurons where the voltage trace was slow to rise or distorted were discarded. The total volume of fluid in the recording dishes was ∼1 ml. The Petri dishes were superfused at a flow rate of 2 ml min^{-1}. Input capacitance (C_{in}) was calculated from the membrane time constant and input resistance or by the integration of the capacitative transient generated by a 10 mV voltage step (Abdulla & Smith, 1997*a*,*b*). In current-clamp, external solution contained (in mM): 127 NaCl, 2.5 KCl, 1.2 NaH_2PO_4, 26 $NaHCO_3$, 2.5 $CaCl_2$, 1.3 $MgSO_4$ and 25 D-glucose saturated with 95% O_2–5% CO_2. Internal (pipette) solution contained (in mM): 130 potassium gluconate, 4 Mg-ATP, 0.3 Na-GTP, 10 EGTA, 2 $CaCl_2$ and 10 Hepes (adjusted to pH 7.2 with KOH; osmolarity 310–320 mosmol l^{-1}). Current-clamp recordings were made at resting membrane potential (RMP). All-points histograms (Li & Baccei, 2011) were generated by assigning the original digital points into 10 mV bins. These were used to summarize and describe action potential (AP) discharge in responses to a 450 ms current ramp to 2 nA.

Na^+ channel current (I_{Na}) was recorded in an external solution containing the following (in mM): 75 TEA-Cl, 50 NaCl (to improve voltage-clamp control), 5 KCl, 4 $MgCl_2$, 10 Hepes and 60 D-glucose (adjusted to pH 7.4 with NaOH; osmolarity 330 mosmol l^{-1}). Internal solution contained the following (in mM): 140 CsCl, 10 NaCl, 2 MgATP, 0.3 Na_2GTP, 2 EGTA, 10 Hepes and 2 $MgCl_2$ (adjusted to pH 7.2 with NaOH; osmolarity 300–310 mosmol l^{-1}). Tetrodotoxin (TTX) (Alomone Labs, Jerusalem, Israel) (300 nM) was applied by superfusion. Total I_{Na} was recorded in response to 40 ms depolarizing voltage commands from a holding potential (V_h) of −90 mV and leak subtracted by means of a *P*/6 protocol. Thus, a series of one-sixth amplitude, reversed polarity voltage commands were applied, and the recorded currents multiplied by 6 and added to the recordings of I_{Na}. Current decay (fast inactivation) was fitted with a single exponent function:

$$f(t) = \sum_{i=1}^{n} Aie^{-t/\tau i} + C$$

For voltage dependence of activation, normalized (I/I_{-20}) *I*–*V* curves were fitted with a single Boltzmann function, $y = A_2 + (A_1 - A_2)/(1 + \exp((x - x_0)/dx))$. The I_{Na} steady-state fast inactivation protocol involved 300 ms prepulses increasing from −110 mV followed by 10 ms test pulses to −10 mV to determine the fraction of current available (I/I_{-110}). The I_{Na} steady-state slow inactivation protocol involved application of 5 s prepulses, followed by 20 ms recovery pulses to −120 mV (to allow recovery from fast inactivation), followed by 10 ms test pulses to −10 mV to determine the fraction of current available (I/I_{-120}). To obtain the TTX- resistant and -sensitive (TTX-R and TTX-S, respectively) components of the current, currents persisting in the presence of 300 nM TTX (TTX-R I_{Na}) were subtracted from the corresponding values of total I_{Na} to reveal TTX-S I_{Na}.

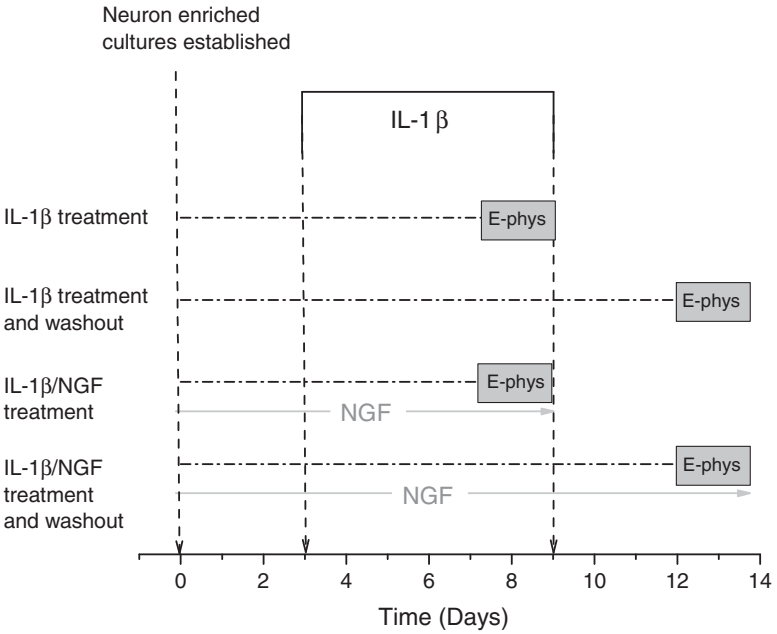

Figure 1. Scheme to show time course of exposure of cultured neurons to IL-1β and NGF
Relevant control experiments for each experimental protocol were carried out with the omission of IL-1β.

For recording K^+ channel currents, external solution contained (in mM): 145 *N*-methyl-D-glucamine (NMG)-Cl, 10 KCl, 2.5 $CaCl_2$, 10 Hepes, 1.0 $MgCl_2$ and10 D-glucose (adjusted to pH 7.4 with HCl; 320 mosmol l^{-1}). Internal solution contained (in mM): 100 potassium gluconate, 40 NMG-Cl, 2 Mg-ATP, 0.3 Na_2GTP, 11 EGTA, 10 Hepes and 0.1 $CaCl_2$ (adjusted to pH 7.2 with HCl; 300 mosmol l^{-1}). In view of the complexity and variability of potassium currents in DRG neurons (Gold *et al.* 1996; Everill & Kocsis, 1999) a relatively simplified approach was used for their isolation. Total K^+ channel current (I_K) was recorded at voltages between −60 mV and +60 mV following a 500 ms conditioning prepulse (V_p) to −120 mV or −30 mV and leak subtracted by means of a *P*/6 protocol. Voltage commands were then repeated in the presence of 5 mM Mn^{2+} to reveal Mn^{2+}-resistant I_K. Digital subtraction of Mn^{2+}-resistant I_K (V_p = −120 mV) from the total I_K (V_p = −120 mV) yielded Mn^{2+}-sensitive I_K, which corresponded to the total Ca^{2+}-sensitive K^+ conductance ($I_{K,Ca}$) (Abdulla & Smith, 2001*b*). I_A type K^+ currents were obtained by subtracting Mn^{2+}-resistant I_K recorded following a −30 mV prepulse from that recorded following a −120 mV prepulse.

I_{Ca} was measured using Ba^{2+} as a charge carrier (I_{Ba}). For these experiments, external 'Ba^{2+}' solution contained (in mM): 160 TEA-Cl, 10 Hepes, 2 $BaCl_2$, 10 D-glucose and 300 nM TTX (adjusted to pH 7.4 with TEA-OH; osmolarity 330–340 mosmol l^{-1}). Internal solution contained (in mM): 120 CsCl, 5 Mg-ATP, 0.4 Na_2-GTP,10 EGTA and 20 Hepes (adjusted to pH 7.2 with CsOH; osmolarity 300–310 mosmol l^{-1}). I_{Ba} was evoked using a series of 150 ms depolarizing voltage commands from V_h = −100 mV or V_h = −60 mV and leak subtracted by means of a *P*/6 protocol. For the voltage dependence of I_{Ba} inactivation, the fraction of current available at command potential (V_{cmd}) = −10 mV was determined in response to a series of 3.5 s incremental prepulses from V_h = −110 mV. Normalized (I/I_{-110}) inactivation curves were fitted with a single Boltzmann function, $y = A_2 + (A_1 - A_2)/(1 + \exp((x - x_0)/dx))$.

Current through hyperpolarization-activated cyclic nucleotide-gated (HCN) channels (I_H) was recorded in an external solution containing the following (in mM): 150 NaCl, 5 KCl, 2.5 $CaCl_2$,1 $MgCl_2$, 10 Hepes and 10 D-glucose (adjusted to pH 7.4 with NaOH; osmolarity 330–340 mosmol l^{-1}). Internal solution contained (in mM): 130 potassium gluconate, 2 Mg-ATP, 0.3 Na-GTP, 11 EGTA, 10 Hepes and 1 $CaCl_2$ (adjusted to pH 7.2 with KOH; osmolarity 310–320 mosmol l^{-1}). I_H was elicited by a series of hyperpolarizing voltage commands (from −60 mV to −130 mV) that were also decremental in duration (from 4.25 s to 2.5 s) from a V_h of −50 mV. The time course for the activation of I_H was fitted with the sum of a two exponential function:

$$f(t) = \sum_{i=1}^{n} Aie^{-t/\tau i} + C$$

For the voltage dependence of activation, the conductance ratio, G/G_{-130}, was calculated from tail current ($I_{H,Tail}$) amplitudes measured 100–200 ms after repolarization and curves were fitted with a single Boltzmann function, $y = A_2 + (A_1 - A_2)/(1 + \exp((x - x_0)/dx))$.

Analysis and statistics

All electrophysiological data were acquired and analysed using pCLAMP10 software (Axon Instruments/Molecular Devices). Figures were produced with Origin 9.1 (OriginLab, Northampton, MA, USA). Where applicable, data are presented as means ± standard error of the mean (SEM). Statistical comparisons were made with Student's unpaired *t* test or Fisher's exact test. *P* values from these statistical tests were determined using GraphPad Prism 5.00 (GraphPad Software, San Diego, CA, USA). Statistical significance was taken as $P < 0.05$.

Results

Effects of long-term IL-1β exposure on neuronal excitability

We used all-points histograms (Li & Baccei, 2011) to illustrate and clarify our previous observation that the excitability of medium diameter rat DRG neurons increases after 5–6 days of exposure to 100 pM IL-1β (Stemkowski & Smith, 2012*a*). The original digital points used to describe action potential (AP) discharge in response to a 450 ms current ramp to 2 nA were assigned to 10 mV bins starting at −20 mV (Fig. 2*A*). We collected and pooled 2500 digital points from each of 19 control, medium-diameter neurons and from 19 others exposed to cytokine. The presence of more points in all bins positive to −25 mV is indicative of increased AP discharge in the continued presence of IL-1β (Fig. 2*C*). To better quantify this effect on a neuron-by-neuron basis, we counted the number of data points occurring above −25 mV in each of 29 control neurons and 22 IL-1β treated medium neurons. Since different acquisition rates were used for some of these neurons, data were expressed as the percentage of points above −25 mV. The mean percentage of points acquired in the IL-1β treated neurons was significantly greater that that obtained from control neurons (Fig. 2*D*, $P < 0.05$). Sample recordings to illustrate IL-1β induced increases in excitability are shown in Fig. 2*E* and *F*.

IL-1β-induced changes in single action potential parameters in medium neurons were dominated by a decrease in AP afterhyperpolarization (AHP) and increase in spike height (Fig. 2*B*). Although full numerical data and statistics are presented in our previous publication (Stemkowski & Smith, 2012*a*), this presentation of the data was obtained by averaging the original AP recordings from 12 control neurons and 12 treated with IL-1β.

Reversibility of IL-1β effects

If the above actions of IL-1β reflect the initiation of a long-term or even a permanent change in the electrophysiological phenotype of medium neurons, they should persist when the cytokine is removed. To test this possibility, we exposed 25 medium neurons to IL-1β for 5–6 days and then examined excitability after a further

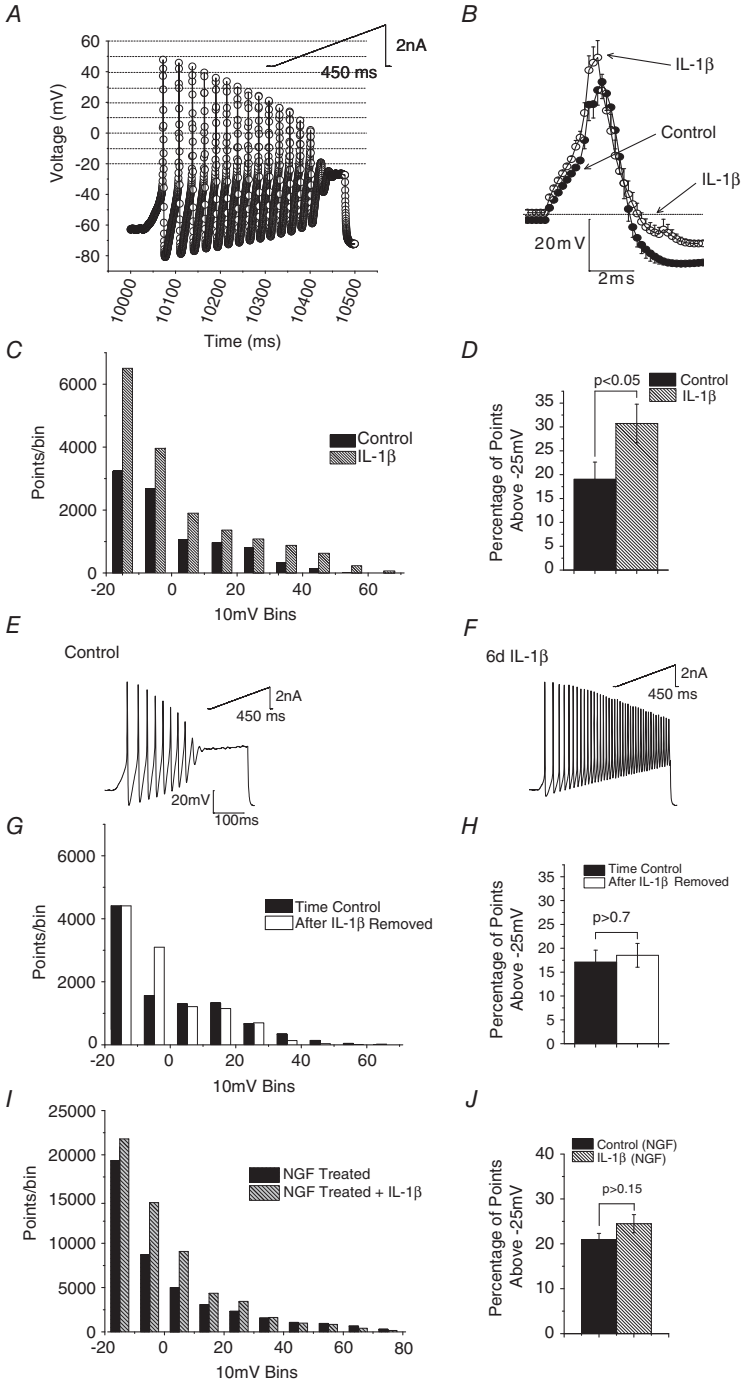

Figure 2. Long-term IL-1β exposure reversibly increases DRG neuron excitability
A, depiction of original digital points used to describe AP discharge in a medium-sized neuron in response to 450 ms depolarizing current ramp to +2.0 nA (inset). Digital points were assigned to 10 mV bins, starting at −20 mV and shown by dotted lines in the figure. *B*, averaged AP waveforms from 12 control medium-diameter neurons and 19 neurons exposed to IL-1β for 5–6 days. Note increase in spike height and attenuation of AHP. *C*, all points histogram derived from 2500 digital points collected from 19 control medium-diameter neurons and from 19 others exposed to cytokine. Note the presence of more points in bins positive to −25 mV. *D*, increase in percentage of points above −25 mV in the continued presence of IL-1β indicative of increased AP discharge (data from 29 control neurons and 22 in the presence of IL-1β, $P < 0.05$ Student's *t* test). *E* and *F*, sample data records of discharge evoked by 450 ms ramps to 2 nA in a control neuron and one exposed to IL-1β for 6 days. *G*, all points histogram to show lack of long lasting change in excitability as a consequence of 5–6 days of IL-1β exposure. Points from 25 control neurons which were maintained in culture for 12–14 days without exposure to cytokine and from 25 neurons examined 3–4 days after a previous 5–6 days of exposure to IL-1β. Data from 8000 data points obtained from responses to 250 ms ramps to +2.0 nA. *H*, comparison of the percentage of digital points in each neuron above −25 mV reveals no persistent increase in excitability as a result of IL-1β exposure and removal ($P > 0.7$). *I*, all points histogram to show lack of effect of 5–6 days of IL-1β exposure on neurons treated with NGF (50 ng ml^{-1}). Points from 30 neurons which were maintained in culture in the presence of NGF and from another 30 NGF-treated neurons examined 3–4 days after a previous 5–6 days of exposure to IL-1β (refer to Fig. 1). Data from 8000 data points obtained from responses to 250 ms ramps to +2 nA. *J*, comparison of the percentage of digital points in each neuron above −25 mV reveals no increase in excitability of NGF treated neurons in response to 5–6 days of IL-1β exposure ($P > 0.7$). Error bars in *B*, *D*, *H* and *J* represent SEM.

3–4 days (see Fig. 1). The control data were obtained from another 25 untreated neurons left for a total of 12–14 days in culture. All-points histogram data from 8000 points per neuron are shown in Fig. 2*G*. For most 10 mV bins (apart from the −10 mV bin), the number of points acquired from control neurons does not appear to differ from those treated with IL-1β. The effects of 5–6 days of exposure to IL-1β thus reverse within 3–4 days. This is supported by the analysis of the same data shown in Fig. 2*H*, which shows the mean percentage of digital points in each cell recorded above −25 mV. There is no difference between points acquired from control neurons ($n = 25$) and points acquired from neurons that had previously received a transient 5–6 days of exposure to IL-1β ($n = 25$, $P > 0.7$).

Rationale for omission of NGF from cultures

Culture protocols for DRG neurons often involve the inclusion of NGF as this is required for maintenance of normal neuronal phenotypes (Chalazonitis *et al.* 1987; Dib-Hajj *et al.* 1998; Everill & Kocsis, 2000). There is however documented overlap of the downstream signalling pathways engaged by IL-1β and NGF. For example, the Ras-MAPK pathway (Kaplan & Stephens, 1994) and ERK1/2 phosphorylation (Yang *et al.* 2013) are activated by both ligands. We used immunoblots to confirm that IL-1β promotes phosphorylation of ERK1 and ERK2 in DRG neuron cultures (Stemkowski, Smith and Posse de Chaves, unpublished observations). We also found that inclusion of NGF (50 ng ml^{-1}, 5 days, see Fig. 1) greatly increased medium cell excitability and occluded effects of IL-1β. Thus in all-points histograms obtained from voltage responses to current ramps, there is no significant difference in the percentage of points above −25 mV between NGF treated neurons ($n = 30$) and neurons treated with NGF plus IL-1β ($n = 30$, $P > 0.15$, Fig. 2*I* and *J*). In view of these findings, we omitted NGF from our cultures when studying effects of IL-1β on ionic currents. These findings can thus be directly related to our previous studies of effects of IL-1β on excitability where NGF was also omitted (Stemkowski & Smith, 2012*a*).

Effects of long-term IL-1β exposure on I_{Na}

Total I_{Na} was recorded from medium-diameter DRG neurons in NGF-free defined medium culture using a series of 40 ms depolarizing voltage commands from $V_h = -90$ mV (Fig. 3*Aa*). To improve voltage-clamp control, Na^+ concentration in the external solution was reduced to 50 mM. Using a Cs^+ based electrode solution to block K^+ currents, neurons were then treated with 300 nM TTX to isolate TTX-S I_{Na} from TTX-R I_{Na} (Fig. 3*Ab*). Digital subtraction (Fig. 3*Ac*) reveals that, under these NGF-free culture conditions, all measurable current in all 20 medium-diameter neurons was TTX-S I_{Na}.

Effects of IL-1β on TTX-S I_{Na} density were generally very modest. The *I–V* plot in Fig. 3*B* appears to show that TTX-S I_{Na} for IL-1β treated medium-diameter neurons is actually smaller than control at voltage commands between −10 mV and +20 mV but this difference is not significant ($0.05 < P \leq 0.1$, unpaired *t* test). However, peak TTX-S I_{Na} occurred at −20 mV for control neurons (-261 ± 48 pA pF^{-1}, $n = 9$), but at −30 mV for neurons exposed to IL-1β (-176 ± 44 pA pF^{-1}, $n = 11$, Fig. 3*B*). Consistent with this finding, single Boltzmann function fitting of the curves for the voltage dependence of activation revealed that the average voltage midpoint ($V_{1/2}$) was significantly shifted leftward (hyperpolarizing shift in TTX-S I_{Na} activation) after long-term IL-1β exposure (from -32.5 ± 2.6 mV, $n = 9$ to -41.4 ± 2.2 mV, $n = 11$; $P < 0.05$, unpaired *t* test; Fig. 3*C*, also see Table 1). By contrast with g_{Na} activation, IL-1β exposure failed to produce a significant shift in the curves for fast or slow inactivation (Fig. 3*C* and *D*, respectively). Single exponential fits of TTX-S I_{Na} decay in medium-diameter neurons revealed no differences in the kinetics for fast inactivation in response to IL-1β treatment (Fig. 3*E*).

Effects of long-term IL-1β exposure on K^+ currents

By contrast with its rather weak actions on I_{Na} (Fig. 3), I_{Ca} and I_H (see below), IL-1β promoted profound suppression of K^+ currents. Voltage-clamp protocols and solutions were designed to examine both voltage- and Ca^{2+}-dependent K^+ currents ($I_{K,Ca}$), since reductions in these currents are implicated in increased sensory neuron excitability and broadening of APs following peripheral nerve injury (Everill & Kocsis, 1999; Abdulla & Smith, 2001*b*; Kim *et al.* 2002). Since at least six types of K^+ current can be recorded in the cell bodies of DRG neurons (Gold *et al.* 1996), we used a simplified approach to investigate the effects of long-term IL-1β exposure. We recorded total I_K and Mn^{2+}-resistant I_K, and obtained Mn^{2+}-sensitive I_K and I_A by subtraction and/or by adjusting holding potential (V_h).

Figure 4*Aa* illustrates total I_K evoked by a series of depolarizing voltage commands from −120 mV in a medium-sized DRG neuron. Figure 4*Ab* illustrates Mn^{2+}-resistant I_K recorded in the same neuron in the presence of 5 mM Mn^{2+}. Figure 4*Ac* is the subtraction of records in Fig. 4*Ab* from those in Fig. 4*Aa* to reveal Mn^{2+}-sensitive I_K, which corresponds to $I_{K,Ca}$. Figure 4*Ba* illustrates Mn^{2+}-resistant I_K recorded from −120 mV in another neuron and Fig. 4*Bb* illustrates Mn^{2+}-resistant currents recorded in the same neuron following a prepulse to −30 mV. Subtraction of recordings in Fig. 4*Bb* from those in Fig. 4*Ba* reveals a rapidly activating/rapidly inactivating current that we have termed I_A, recognizing that it may reflect activation of multiple channel types (Gold *et al.* 1996).

IL-1β produced profound suppression of Mn^{2+}-resistant I_K in medium-sized neurons (Fig. 4*C*). Thus at +60 mV, steady-state current density was reduced from 169 ± 25 pA pF^{-1}, $n = 9$ to 62 ± 10 pA pF^{-1}, $n = 16$ ($P < 0.001$, unpaired t test, Fig. 4*C*; a ∼64% decrease). Figure 4*D* illustrates representative records of Mn^{2+}-resistant I_K recorded at +60 mV in the absence or presence of IL-1β.

Ninety per cent (9/10) of control and 94% (15/16) of IL-1β treated medium-diameter neurons had measurable

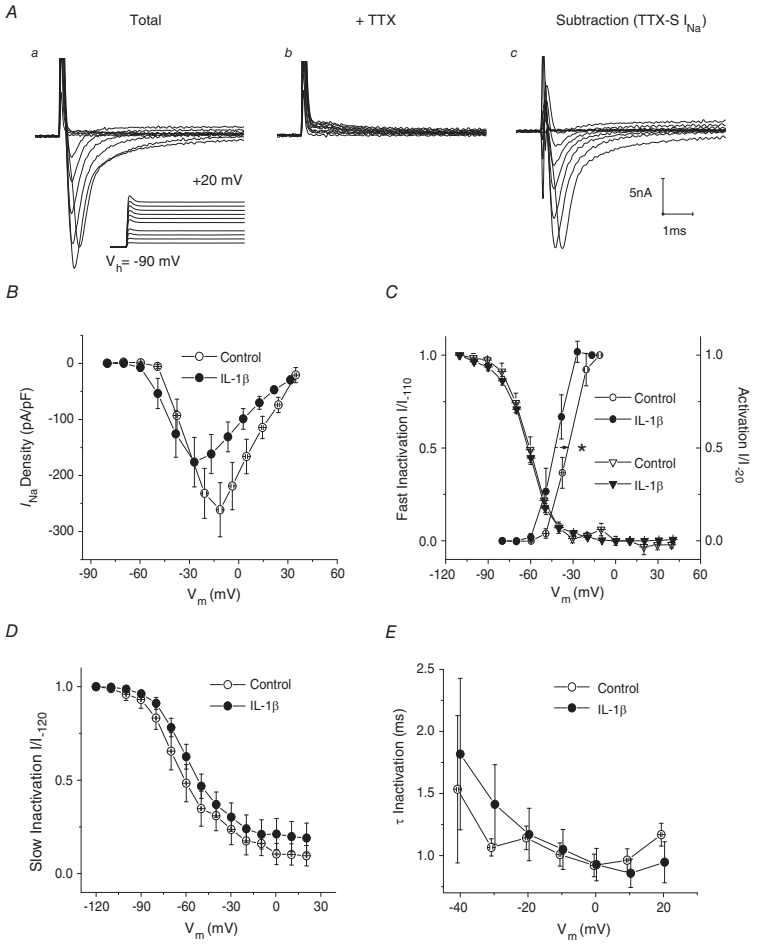

Figure 3. Five to six days of IL-1β exposure increases the availability of TTX-S I_{Na} in medium-diameter DRG neurons

A, I_{Na} recorded before and after superfusion of 300 nM TTX. Digital subtraction of currents in *Ab* from those in *Aa* reveals that all measurable current in medium-diameter neurons cultured in the absence of NGF was TTX-S I_{Na} (*Ac*). Voltage recordings corresponding to the recorded currents are shown in the lower record of *Aa*. *B*, current–voltage plot. TTX-S I_{Na} density for IL-1β treated medium-diameter neurons was not significantly different from control ($0.05 < P \leq 0.1$) at voltage commands between −10 mV and +20 mV. However, peak TTX-S I_{Na} occurred at $V_{cmd} = -20$ mV for control neurons (−261 ± 48 pA pF^{-1}, $n = 9$), whereas peak current density occurred at −30 mV for neurons exposed to IL-1β (−176 ± 44 pA pF^{-1}, $n = 11$). *C*, normalized activation (I/I_{-20}) curves (circles) were fit with a single Boltzmann function. IL-1β produced a significant hyperpolarizing shift on values for $V_{1/2}$ (from −32.5 ± 2.6 mV, $n = 9$ to −41.4 ± 2.2 mV, $n = 11$). Slope factor was unaffected (control, 3.6 ± 1.1 mV, $n = 9$ *vs*. IL-1β: 3.3 ± 0.5 mV, $n = 11$). Single Boltzmann function fits of steady-state fast inactivation (I/I_{-110}) curves (triangles) reveal that IL-1β had no significant effect on values for $V_{1/2}$ (control, −61.3 ± 1.9 mV, $n = 7$ *vs*. IL-1β: −62.0 ± 0.9 mV, $n = 11$) or slope factor (control, 7.7 ± 0.8 mV, $n = 7$ *vs*. IL-1β: 8.8 ± 0.9 mV, $n = 11$). *D*, single Boltzmann function fits of normalized steady-state slow inactivation (I/I_{-120}) curves reveal that IL-1β had no significant effect on values for $V_{1/2}$ (control, −62.4 ± 6.1 mV, $n = 5$ *vs*. IL-1β: −57.8 ± 2.5 mV, $n = 5$; $P > 0.05$) or slope factor (control, 13.5 ± 1.9 mV, $n = 5$ *vs*. IL-1β: 13.6 ± 1.1 mV, $n = 5$). *E*, single exponential fits of TTX-S I_{Na} decay reveal no differences in the kinetics for fast inactivation in response to IL-1β treatment ($V_{cmd} = -40$ mV; control, 1.53 ± 0.59 ms, $n = 5$ *vs*. IL-1β: 1.82 ± 0.61 ms, $n = 11$). Error bars indicate means ± SEM. Significant difference *versus* control $^*P < 0.05$ with unpaired t test. Traces in *A* were not subtracted for leak current. V_m in panels *B–E* refers to recorded membrane voltage.

Table 1. Summary of single Boltzmann function parameters in control *versus* IL-1β treated medium-diameter DRG neurons

Parameter	Control	IL-1β
I_{Na} activation $V_{1/2}$ (mV)	−32.5 ± 2.6 mV (9)	−41.4 ± 2.2 mV (11)*
I_{Na} activation slope factor (mV)	3.6 ± 1.1 mV (9)	3.3 ± 0.5 (11)
I_{Na} steady-state fast inactivation $V_{1/2}$ (mV)	−61.3 ± 1.9 mV (7)	−62.0 ± 0.9 (11)
I_{Na} steady-state fast inactivation slope factor (mV)	7.7 ± 0.8 mV (7)	8.8 ± 0.9 (11)
I_{Na} steady-state slow inactivation $V_{1/2}$ (mV)	−62.4 ± 6.1 mV (5)	−57.8 ± 2.5 (5)
I_{Na} steady-state slow inactivation slope factor (mV)	13.5 ± 1.9 mV (5)	13.6 ± 1.1 (5)
I_{Ba} inactivation $V_{1/2}$ (mV)	−45.3 ± 13.8 mV (7)	−78.8 ± 5.9 (13)*
I_{Ba} slope factor (mV)	15.0 ± 2.2 mV (7)	17.8 ± 1.4 (13)†
I_H steady-state activation $V_{1/2}$ (mV)	−70.7 ± 2.7 mV (9)	−65.9 ± 5.1 mV (10)
I_H slope factor (mV)	12.2 ± 1.6 mV (9)	10.7 ± 1.7 (10)

Values are means ± SEM (n). Significant difference *versus* control $^*P < 0.05$ and $^\dagger P < 0.01$ with unpaired t test.

I_A ($P > 0.05$, Fisher's exact test). Similar to Mn^{2+}-resistant I_K (Fig. 4*C*), there was a significant reduction in I_A density (for example, at +60 mV I_A density was reduced from a control value of 31 ± 9 pA pF^{-1}, $n = 10$ to 13 ± 4 pA pF^{-1}, $n = 16$ in the presence of IL-1β; $P < 0.05$, unpaired t test; Fig. 4*E*; an ∼68% decrease). Figure 4*F* illustrates representative records of I_A recorded at +60 mV in the presence and absence of IL-1β.

IL-1β exposure also reduced Mn^{2+}-sensitive I_K density. Thus at +60 mV, current density was reduced from 98 ± 16 pA pF^{-1}, $n = 12$ to 51 ± 10 pA pF^{-1}, $n = 16$ ($P < 0.05$, unpaired t test; Fig. 4*G*; a ∼36% decrease). Further, at command voltages between −30 mV and +10 mV, IL-1β reduced the size of the characteristic of $g_{K,Ca}$ 'hump' in the N-shaped I–V curve (Fig. 4*G*) Figure 4*H* illustrates representative records of Mn^{2+}-sensitive I_K recorded at +60 mV in the presence and absence of IL-1β.

Figure 4*C*, *E* and *G* also illustrates that IL-1β failed to affect membrane resistance at potentials between −60 and −30 mV, indicating no effect on leak conductance as might be expected from the lack of effect of cytokine on the RMP of medium-diameter neurons (Stemkowski & Smith, 2012*a*). These findings (Fig. 4*C*–*H*) do nevertheless imply that IL-1β attenuated delayed rectifier K^+ currents (i.e. Mn^{2+}-resistant I_K), as well as I_A and $I_{K,Ca}$.

Effects of long-term IL-1β exposure on I_{Ca}/I_{Ba}

Ba^{2+} was substituted for Ca^{2+} as the charge carrier, and currents (I_{Ba}) were evoked using a series of 150 ms depolarizing voltage commands from −100 mV or from a holding potential reflective of their normal RMP ($V_h = -60$ mV). The I–V plots shown in Fig. 5*A* were obtained using $V_h = -100$ mV. From this voltage, 5–6 days of IL-1β treatment significantly increased medium neuron I_{Ba} densities at command voltages between −40 mV and −20 mV (unpaired t test, $P < 0.01$). High voltage activated (HVA)-I_{Ba} peak current density (recorded at $V_m = -10$ mV) in the presence of IL-1β (−154 ± 12 pA pF^{-1}, $n = 14$) appeared larger than that recorded in control cultures (−107 ± 22 pA pF^{-1}, $n = 9$), but this effect fell just short of attaining significance (unpaired t test, $0.05 < P \leq 0.1$).

By contrast, IL-1β caused a significant reduction in peak I_{Ba} density in medium-diameter DRG neurons when currents were evoked from $V_h = -60$ mV. At −10 mV, I_{Ba} was reduced from 58 ± 6 pA pF^{-1}, $n = 10$ to 38 ± 4 pA pF^{-1}, $n = 11$ ($P < 0.01$, unpaired t test; Fig. 5*B*). Unlike our previous studies of acutely dissociated medium-diameter neurons (Abdulla & Smith, 2001*b*), we were unable to detect appreciable T-type Ca^{2+} currents using $V_h = -100$ mV under the culture conditions that were employed.

To examine the possibility that reductions in the peak density of I_{Ba} seen when $V_h = -60$ mV are related to an effect of IL-1β on the voltage dependence of inactivation, the fraction of current available at −10 mV was determined following a series of 3.5 s prepulses to potentials between −110 and −20 mV. Recordings from a typical experiment are illustrated in Fig. 5*C*. Although peak I_{Ba} density recorded at −10 mV from $V_h = -100$ mV was 51.57 ± 9.6 pA pF^{-1} ($n = 9$) and this was unchanged in the presence of IL-1β (58.52 ± 8.0 pA pF^{-1}; $n = 13$, $P > 0.5$), there was a significant shift in $V_{1/2}$ from a control value of −45.3 ± 13.8 mV ($n = 7$) to −78.8 ± 5.9 mV ($n = 13$) for IL-1β treated neurons ($P = 0.02$). Slope factor was unaffected (15.0 ± 2.2 mV, $n = 7$ for control neurons compared with 17.8 ± 1.4 mV, $n = 13$ for IL-1β treated neurons; $P = 0.27$; Fig. 5*D* and Table 1). These findings imply that IL-1β may affect both density and inactivation of HVA I_{Ca}/I_{Ba} but close to the normal resting potential of medium neurons (−60 mV), the effect of increased inactivation dominates so that the amplitude of the observed current is decreased.

Effects of long-term IL-1β exposure on I_H

Hyperpolarization-activated cation currents (I_H) carried by HCN channels are present in many types of DRG

neuron (Mayer & Westbrook, 1983; Scroggs *et al.*1994; Abdulla & Smith, 2001*b*; Emery *et al.* 2011). Since increases in I_H in DRG neurons have been associated with various types of peripheral nerve injury (Chaplan *et al.* 2003; Yao *et al.* 2003; Emery *et al.* 2011), the effect of long-term IL-1β exposure on I_H was examined. From $V_h = -50$ mV, I_H was elicited by a series of incremental, hyperpolarizing voltage commands (from −60 to −130 mV) that were decremental in duration (from 4.25 to 2.5 s; Fig. 6*A*). This voltage protocol was designed to maximize capture of steady-state I_H activation, yet provide stable voltage-clamp recordings at very negative voltages. All 10 control medium-diameter

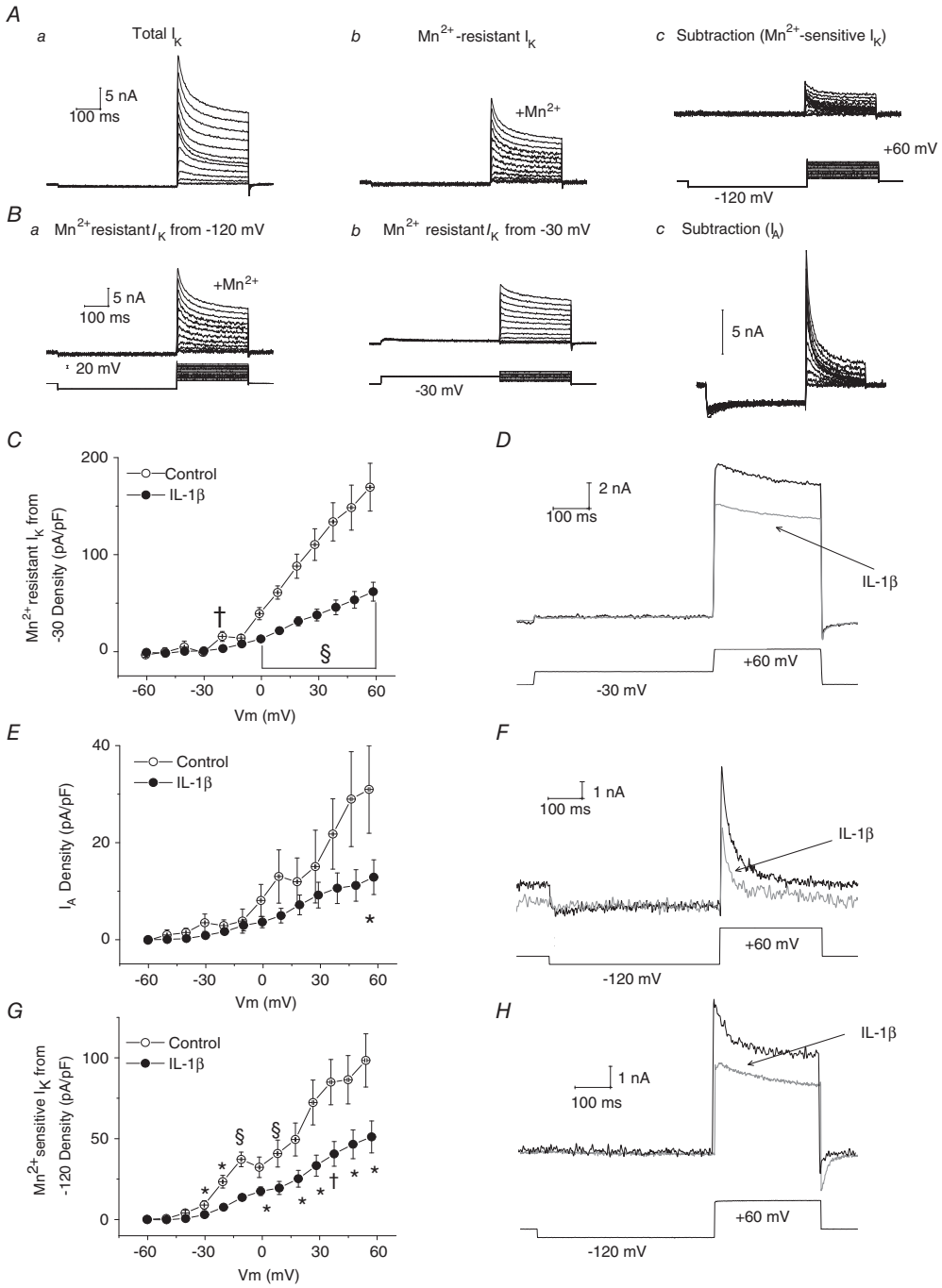

Figure 4. Five to six days of IL-1β exposure decreases I_A density, as well as Mn^{2+}-resistant and Mn^{2+}-sensitive I_K densities in medium-diameter DRG neurons
Aa, family of total outward K^+ currents recorded at voltages between −60 mV and +60 mV after a 500 ms conditioning prepulse to −120 mV. *Ab*, responses of the same neuron as in *Aa* to the same series of voltage

neurons that were studied exhibited a robust I_H at −90 mV (342 ± 91pA, n = 10). As reported by Abdulla & Smith (2001*b*), the inward current consisted of an initial instantaneous current (I_{INST}), followed by slower inward relaxation (I_H) that became larger and that developed more rapidly at more negative voltages (Fig. 6*A* and *B* inset). Although the averaged *I–V* plots shown in Fig. 6*B* appear to show that exposure to IL-1β increases I_H density in medium-diameter neurons at voltage commands between −60 and −90 mV, these differences were not significant (V_{cmd} = −80 mV; from −6 ± 1 pA pF^{-1} in control neurons, n = 9 to −11 ± 2 pA pF^{-1}, n = 12 in IL-1β treated neurons; $0.05 < P \leq 0.1$, unpaired t test). The effect of IL-1β on steady-state activation for I_H was also examined. As described by Kouranova *et al.* (2008), the conductance ratio, g/g_{-130}, was calculated from tail current ($I_{H,Tail}$) amplitudes measured 100–200 ms after repolarization (Fig. 6*C* inset) and g–V relationships for I_H steady-state activation were then plotted (Fig. 6*C*). The averaged g–V curves, however, are nearly superimposed and single Boltzmann function fitting of the steady-state activation curves for I_H reveals that IL-1β exposure had no significant effect on the values for $V_{1/2}$ of activation (control, −70.7 ± 2.7 mV, n = 9 *vs.* IL-1β, −65.9 ± 5.1, n = 10; $P > 0.05$, unpaired t test; Fig. 6*C*, also see Table 1) or slope factor (control, 12.2 ± 1.6 mV, n = 9 *vs.* IL-1β, 10.7 ± 1.7 mV, n = 10; $P > 0.05$, unpaired t test).

Despite the lack of a significant effect on I_H density (Fig. 6*B*) and steady-state activation (Fig. 6*C*), IL-1β produced a clear effect on activation kinetics. Current onset was measured as the sum of two exponential functions as previously described by Kouranova *et al.* (2008). Since some individual I_H traces (particularly those with low current amplitude <−80 pA) were better fitted by a single exponential function, they were omitted from the kinetic analysis. Figure 6*D* and *E* illustrates the voltage dependence of fast (τ_{fast}) and slow (τ_{slow}) time constants, respectively. Activation becomes faster toward negative voltages in both control neurons and those exposed to IL-1β. However, both fast and slow time constants became significantly decreased in IL-1β treated cell cultures over a command voltage range that overlapped with the greatest differences in I_H densities (V_{cmd} = −70 mV τ_{fast}; control, 570.5 ± 92.0 ms, n = 5 *vs.* IL-1β, 294.0 ± 45.1 ms, n = 11; $P < 0.01$, unpaired t test; Fig. 6*D*; and V_{cmd} = −70 mV τ_{slow}; control, 4592.3 ± 1114.4 ms, n = 5 *vs.* IL-1β, 1800.4 ± 421.9 ms, n = 11; $P < 0.05$, unpaired t test; Fig. 6*E*). Figure 6*F* shows superimposed sample recordings of I_H recorded from a control medium neuron and an IL-1β treated neuron.

Discussion

Reversibility of IL-1β effect

IL-1β is one of several early pro-inflammatory mediators that are generated by nerve injury. These initiate multiple processes that underlie the onset and chronic persistence of neuropathic pain (Watkins & Maier, 2002; Wolf *et al.* 2006; Gabay *et al.* 2011). To gain further insight into the underlying processes, we exposed neuron enriched DRG cultures to 100 pM IL-1β for 5–6 days as this coincided with the attainment of the peak level of IL-1β seen 7 days after peripheral nerve injury (Nadeau *et al.* 2011). Our results show that IL-1β-induced increases in excitability of medium-sized DRG neurons are reversible. This implies that a direct IL-1β–neuron interaction is not responsible for switching the phenotype of these neurons towards a

commands in the presence of 5 mM Mn^{2+}. *Ac*, subtraction of records in *Ab* from those in *Aa* to reveal Mn^{2+}-sensitive I_K (recordings of membrane voltage shown in lower trace). *Ba*, Mn^{2+}-resistant I_K recorded in another medium-sized neuron in the presence of 5 mM Mn^{2+} from a prepulse potential of −120 mV (recordings of membrane voltage shown in lower trace). *Bb*, recordings of currents evoked in the same neuron in presence of Mn^{2+}, but from a prepulse potential of −30 mV (recordings of membrane voltage shown in lower trace). *Bc*, subtraction of data records in *Bb* from those in *Ba* to yield I_A. *C*, averaged *I–V* curves reveal that Mn^{2+}-resistant I_K densities recorded from a prepulse potential of −30 mV were substantially smaller following exposure to long-term IL-1β with significant reductions at command voltages −20 mV to +60 mV (for example, peak non-inactivating I_K density (V_{cmd} = +60 mV), from +169 ± 25 pA pF^{-1}, n = 9 to +62 ± 10 pA pF^{-1}, n = 16; $P < 0.001$). *D*, representative traces illustrating suppressed Mn^{2+}-resistant I_K in medium-diameter neurons exposed to IL-1β (grey trace) *versus* control (black trace; the voltage recording shown in lower trace is the from control neuron). *E*, *I–V* plot to illustrate that IL-1β also significantly suppressed I_A density (at +60 mV control, +31 ± 9 pA pF^{-1}, n = 10 *vs.* IL-1β, +13 ± 4 pA pF^{-1}, n = 16; $P < 0.05$). *F*, representative traces illustrating suppressed peak I_A in medium-diameter neurons exposed to IL-1β (grey trace) *versus* control (black trace; the voltage recording shown in lower trace is the from control neuron). *G*, averaged *I–V* curves indicate that IL-1β exposure significantly suppressed Mn^{2+}-sensitive I_K densities with significant reductions at command voltages between −40 mV and +60 mV (for example, peak inactivating Mn^{2+}-sensitive I_K density, from +98 ± 16 pA pF^{-1}, n = 12 to +51 ± 10 pA pF^{-1}, n = 16; $P < 0.05$). *H*, representative traces illustrating suppressed peak Mn^{2+}-sensitive I_K in medium-diameter neurons exposed to IL-1β (grey trace) *versus* control (black trace; the voltage recording shown in lower trace is from the control neuron). Error bars indicate means ± SEM. Significant difference *versus* control $*P < 0.05$, $\dagger P < 0.01$ and $\S P < 0.001$ with unpaired t test. Traces in *A* and *B* were not subtracted for leak current. All displayed voltages traces and values of V_m are from recordings of membrane voltage.

permanent state that may favour increased excitability and spontaneous activity. This is not to say that a phenotypic shift does not occur as injury-induced changes in a both mRNA and protein levels in primary afferents have been described extensively (for reviews see Waxman *et al.* 1999; Costigan *et al.* 2009; Waxman & Zamponi, 2014). Our data simply imply that this change is not initiated by the direct effect of IL-1β on neurons.

Our findings do not rule out the possibility that the injury-induced increase in IL-1β triggers enduring increases in the excitability of DRG neurons via indirect processes involving other cell types. For example, another pro-inflammatory cytokine, tumour necrosis factor α (TNF-α) has been shown to polarize macrophages along a continuum toward a detrimental (M1) or a beneficial (M2) state in spinal cord injury (Kroner *et al.* 2014). Although IL-1β levels peak 7 days after sciatic nerve injury, they remain significantly elevated at 14 days post-injury. TNF-α levels also remain elevated at 14 days post-injury (Nadeau *et al.* 2011). Perhaps such levels are sufficient to increase DRG excitability in the long term. The possibility that the continued presence of inflammatory mediators, in addition to an overt phenotypic switch, may be involved in the long term maintenance of elevated DRG excitability is supported by the observation that intrathecal administration of IL-1Ra after the establishment neuropathic pain related behaviours in nerve injured animals is anti-allodynic (Mika *et al.* 2008; Gabay *et al.* 2011). It has also been shown that removal of the sciatic nerve cuff, and presumably irritation to the nerve, in CCI studies (Mosconi–Kruger model) after 1 or 5 days produces considerable attenuation of allodynia 20–30 days after initial placement (Dableh *et al.* 2011).

Properties of neurons in long-term DRG cell cultures

In order to deconstruct a complex system and to address the question of direct actions of IL-1β on neurons, we employed neuron enriched cultures to limit any effects of cytokines mediated indirectly by activation of

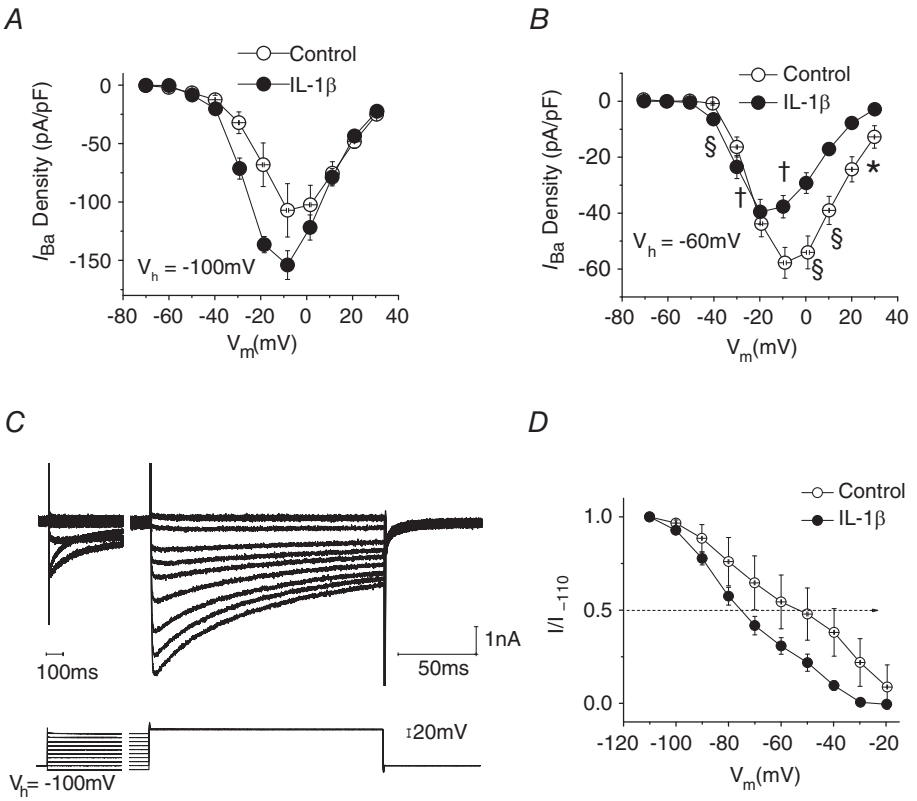

Figure 5. Effects of 5–6 days of IL-1β exposure on I_{Ba} in medium-diameter DRG neurons
A, *I–V* plot shows that IL-1β exposure results in a slight increase in average I_{Ba} density in neurons studied from $V_h = -100$ mV. *B*, by contrast, when $V_h = -60$ mV *I–V* plots reveal a significant reduction in averaged I_{Ba} peak density ($V_{cmd} = -10$ mV) in neurons exposed to IL-1β (from -58 ± 6 pA pF^{-1}, $n = 10$ to -38 ± 4 pA pF^{-1}, $n = 11$; $P < 0.01$). *C*, representative traces illustrating currents and voltage protocols used to determine voltage dependence of inactivation. *D*, single Boltzmann function fitting of curves for the voltage dependence of inactivation reveal that IL-1β exposure led to a significant leftward shift (hyperpolarizing shift in I_{Ba} inactivation) in the values for $V_{1/2}$ (illustrated by dotted line with arrowhead), whereas slope factor was unaffected. Error bars indicate means ± SEM. Significant difference *versus* control $^*P < 0.05$, $^\dagger P < 0.01$ and $^\S P < 0.001$ with unpaired *t* test.

other cell types. The presence of non-neuronal cells in DRG cell cultures and their known expression of IL-1RI (Copray *et al.* 2001) could present a substantial source for the production and release of undefined inflammatory mediators. Despite our attempts to limit growth of non-neuronal cells, both Schwann cells and fibroblasts (Lindsay, 1988) appeared to be present and increased in number with culture duration. Although Schwann

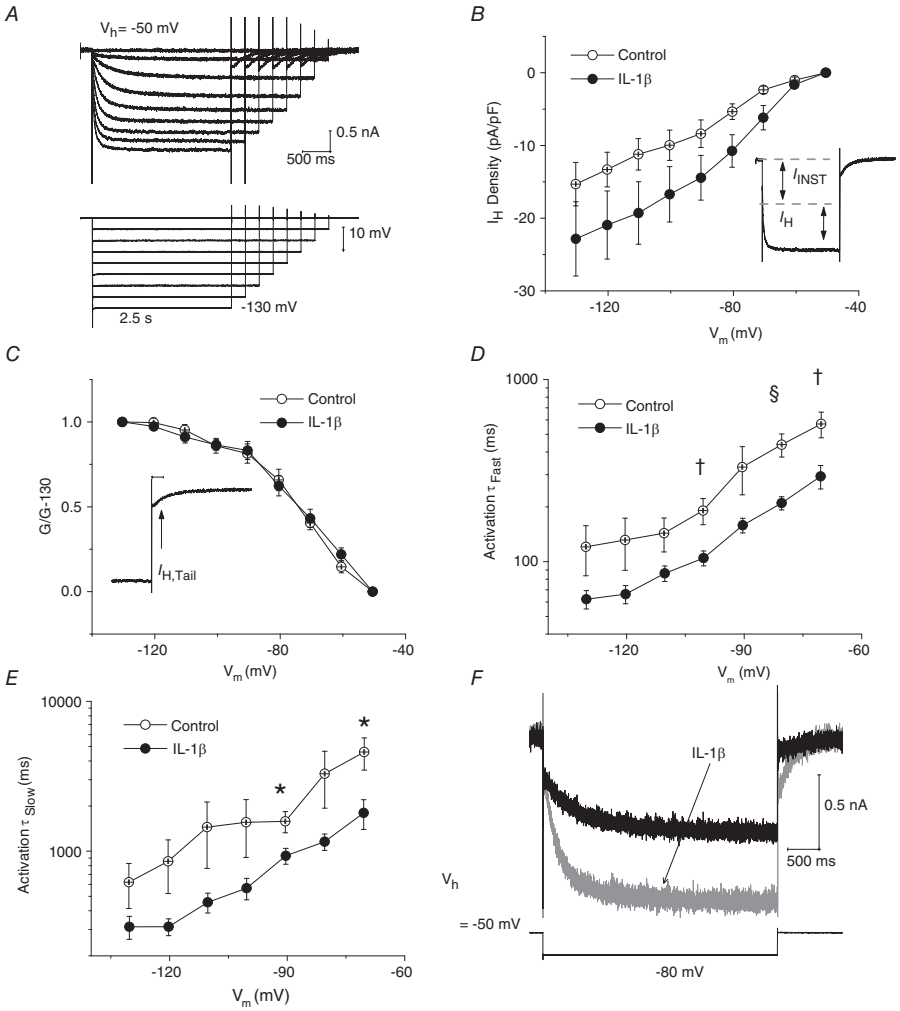

Figure 6. Five to six days of IL-1β exposure increases the availability of I_H in medium-diameter DRG neurons

A, I_H was elicited by a series of incremental hyperpolarizing voltage commands (from −60 mV to −130 mV from V_h = −50 mV). Voltage commands decreased in duration (from 4.25 s to 2.5 s). Voltage trace in lower part of panel is a recording of membrane voltage. *B*, averaged *I–V* plots to illustrate I_H densities (n = 9 for control, n = 12 for recordings in IL-1β). There was no significant difference in I_H density at any of the voltages illustrated. Inset shows that the inward current consisted of an initial instantaneous current (I_{INST}), followed by slower inward relaxation (I_H). *C*, the conductance ratio, g/g_{-130}, was calculated from tail current ($I_{H,Tail}$) amplitudes measured 100–200 ms after repolarization (inset). Single Boltzmann function fitting of steady-state activation curves for I_H reveals that IL-1β had no significant effect on the values for $V_{1/2}$ of activation (control, −70.7 ± 2.7 mV, n = 9 *vs.* IL-1β, −65.9 ± 5.1 mV, n = 10; $P > 0.05$) or slope factor (control, 12.2 ± 1.6 mV, n = 9 *vs.* IL-1β, 10.7 ± 1.7 mV, n = 10; $P > 0.05$). *D*, effect of voltage on fast activation time constant (τ_{fast}). In the presence of IL-1β, the rate of I_H activation was increased. For example, at V_{cmd} = −70 mV τ_{fast} in control, 570.5 ± 92.0 ms, n = 5 *vs.* IL-1β, 294.0 ± 45.1, n = 11; $P < 0.01$. *E*, time constants for I_H activation (τ_{slow}) were also significantly decreased in neurons exposed to IL-1β. For example, at V_{cmd} = −70 mV τ_{slow} in control, 4592.3 ± 1114.4 ms, n = 5 *vs.* IL-1β, 1800.4 ± 421.9, n = 11; $P < 0.05$). *F*, superimposition of a representative trace for a neuron exposed to IL-1β (grey trace) on that of a control neuron (black trace; V_{cmd} = −80 mV; the voltage recording shown in lower trace is from the control neuron). Note that IL-1β increased rates of I_H activation. Error bars indicate means ± SEM. Significant difference *versus* control $^*P < 0.05$, $^\dagger P < 0.01$ and $^\S P < 0.001$ with unpaired t test. Traces in *A* were not subtracted for leak current.

cells can be a source of IL-1β (Watkins & Maier, 1999; Sommer & Kress, 2004), their increased presence was not concurrent with an increase in ambient levels of IL-1β (Stemkowski & Smith, 2012*a*).

Our decision to use defined medium without exogenously added neurotrophins was based on attempting to limit ambient activation of cell signalling pathways, such as MAPKs (MacGillivray *et al.* 2000; Lu *et al.* 2005; Binshtok *et al.* 2008) as these can also be recruited by the activation of the interleukin receptor (IL-1RI). This decision was validated by our finding that IL-1β failed to increase the excitability of NGF treated cultures (Fig 2*I* and *J*) and the unpublished observation that IL-1β promoted ERK phosphorylation in a similar manner to NGF.

Neurons maintained in neurotrophin-free defined medium expressed a slightly different electrophysiological phenotype from those that were acutely isolated (Abdulla & Smith, 2001*b*, 2002). Thus neither T-type Ca^{2+} channel current nor TTX-R I_{Na} were observed under our present conditions. This may not be a major issue as TTX-R I_{Na} makes up only 10% of the total current of acutely isolated medium sized DRG neurons (Abdulla & Smith, 2002). With regard to T-type Ca^{2+} current, it is not clear whether absence in our cultures represents loss of channel expression in otherwise functional DRG neurons, or complete loss of a subpopulation of neurons enriched with T-type Ca^{2+} current. The latter allows for the possibility that the medium-sized neurons supported in our DRG cultures are similar to acutely isolated medium-sized neuron subtypes with inherently less T-type Ca^{2+} current (Abdulla & Smith, 2001*b*).

Effects of IL-1β on ionic currents

Although a multiplicity of changes in various types of K^+, Na^+, Ca^{2+} and HCN channels undoubtedly contribute to increased primary afferent activity after nerve injury (Waxman & Zamponi, 2014) and these changes may reflect the actions of a wide variety of mediators including TNF-α, NGF, BDNF and prostaglandins, (Czeschik *et al.* 2008; Leung & Cahill, 2010; Chen *et al.* 2011; Stemkowski & Smith, 2012*b*), we see relatively weak actions of IL-1β on I_{Na}, I_{Ca} and I_H and find that effects of IL-1β were dominated by decreases in K^+ channel currents. Thus the amplitudes of A-current, delayed rectifier (Mn^{2+}-resistant I_K) and Ca^{2+}-sensitive K^+ currents (Mn^{2+}-sensitive I_K) were reduced by ~68%, ~64% and ~36%, respectively.

It is unlikely that the effects of IL-1β on $I_{K,Ca}$ are secondary to changes in Ca^{2+} influx via Ca^{2+} channels as IL-1β promotes a substantial decrease in $I_{K,Ca}$ recorded from a holding potential of −120 mV (Fig. 4*G* and *H*), yet total I_{Ba} recorded from negative holding potentials may be slightly increased (Fig. 5*A*). Decreases in both the availability of $g_{K,Ca}$ (Abdulla & Smith, 2001*b*; Sarantopoulos *et al.* 2007) and voltage-gated potassium currents (Everill & Kocsis, 1999; Abdulla & Smith, 2001*b*; Kim *et al.* 2002) have been reported in DRG neurons after peripheral nerve injury. These findings may be expected if a persistent low level of IL-1β after the initial peak (Nadeau *et al.* 2011) is responsible for long-term attenuation of K^+ currents after nerve injury.

Mechanisms of IL-1β action

Since the actions of IL-1β are reversible, it is unlikely that enduring alterations in the expression of ion channel protein (auxiliary or pore forming subunits) occur. There may, however, be alterations in ion channel trafficking, membrane insertion or phosphorylation which revert once the cytokine is removed. For example, IL-1β exposure can lead to the activation of extracellular signal regulated kinase (ERK) (Lu *et al.* 2005; Dobierzewska *et al.* 2012), which has been reported to directly phosphorylate specific residues within intracellular loop 1 (L1) of the $Na_V1.7$ sodium channel, thereby allowing sodium channel activation at more hyperpolarized potentials (Stamboulian *et al.* 2010). This would be consistent with our observation for TTX-S I_{Na} shown in Fig. 3*C*. Other kinases may also be recruited, including p38 MAPK (Funakoshi *et al.* 2001; Binshtok*et al.* 2008), which is known to reduce trafficking of K_{Ca} channel subunits to the membrane in chick ciliary ganglion neurons (Chae & Dryer, 2005). Furthermore, the MAPK pathway can regulate the inactivation of HVA I_{Ca} through actions on auxiliary calcium channel subunits (Fitzgerald, 2002). This may account for the shift in inactivation shown in Fig. 5*D*.

IL-1β exposure can also activate protein kinase C (PKC) (Obreja *et al.* 2002; Liu *et al.* 2006) or, through the secondary production of prostaglandin E_2, activate the cAMP/PKA signalling pathway (Maier *et al.*1990; Gray *et al.* 2004). Such activation can suppress A-currents (Hagiwara *et al.* 2003) and $I_{K,Ca}$ (Gold *et al.* 1996*b*; Shipston *et al.* 1999; Widmer *et al.* 2003). cAMP also directly binds to a domain in the C-terminal of the HCN channel (DiFrancesco & Tortora, 1991) which accelerates the opening of HCN2 channels (Wainger *et al.* 2001). All of these possibilities are congruent with our observations on K^+ currents (Fig. 4) and I_H (Fig. 6).

Relationship between current-clamp and voltage-clamp results

The changes in ionic currents in medium-diameter DRG neurons relate to the alterations in AP waveform and the increased cell excitability. The hyperpolarizing shift in voltage dependence of activation of TTX-S I_{Na} (Fig. 3*C*) may contribute to the observed increase in rate of depolarization during the AP upstroke and decreased

rheobase (Stemkowski & Smith, 2012*a*). It may also contribute to the increased spike height (Fig. 2*B*) as more activation of Na^+ conductance may be available prior to the onset of repolarizing K^+ currents, which are themselves attenuated (Fig. 4). Although this global attenuation of K^+ currents in medium neurons is likely to contribute to attenuation of the AP afterhyperpolarization (Fig. 2*B*), the observed increase in rate of activation of I_H (Fig. 6*D*–*F*) may also play a role (Stemkowski & Smith, 2012*a*). Despite the prediction that all observed changes under voltage-clamp conditions are in a direction that would promote increased excitability, more work is clearly required to establish the relationships between altered channel expression and increased excitability. This may be achieved by computer modelling of the voltage trajectories (AP shape and repetitive discharge characterstics) that would be predicted by the observed changes in various ionic conductances.

References

Abdulla FA & Smith PA (1997*a*). Ectopic α_2-adrenoceptors couple to N-type Ca^{2+} channels in axotomized rat sensory neurons. *J Neurosci* **17**, 1633–1641.

Abdulla FA & Smith PA (1997*b*). Nociceptin inhibits T-type Ca^{2+} channel current in rat sensory neurons by a G-protein-independent mechanism. *J Neurosci* **17**, 8721–8728.

Abdulla FA & Smith PA (2001*a*). Axotomy and autotomy-induced changes in the excitability of rat dorsal root ganglion neurons. *J Neurophysiol* **85**, 630–643.

Abdulla FA & Smith PA (2001*b*). Axotomy- and autotomy-induced changes in $Ca^{2+}$and K^+ channel currents of rat dorsal root ganglion neurons. *J Neurophysiol* **85**, 644–658.

Abdulla FA & Smith PA (2002). Changes in Na^+ channel currents of rat dorsal root ganglion neurons following axotomy and axotomy-induced autotomy. *J Neurophysiol* **88**, 2518–2529.

Baccei ML & Kocsis JD (2000). Voltage-gated calcium currents in axotomized adult rat cutaneous afferent neurons. *J Neurophysiol* **83**, 2227–2238.

Baron R, Binder A & Wasner G (2010). Neuropathic pain: diagnosis, pathophysiological mechanisms, and treatment. *Lancet Neurol* **9**, 807–819.

Binshtok AM, Wang H, Zimmermann K, Amaya F, Vardeh D, Shi L, Brenner GJ, Ji RR, Bean BP, Woolf CJ & Samad TA (2008). Nociceptors are interleukin-1β sensors. *J Neurosci* **28**, 14062–14073.

Chalazonitis A, Peterson ER & Crain SM (1987). Nerve growth factor regulates the action potential duration of mature sensory neurons. *Proc Natl Acad Sci USA* **84**, 289–293.

Chae KS & Dryer SE (2005). The p38 mitogen-activated protein kinase pathway negatively regulates Ca2+-activated K+ channel trafficking in developing parasympathetic neurons. *J Neurochem* **94**, 367–379.

Chaplan SR, Guo HQ, Lee DH, Luo L, Liu C, Kuei C, Velumian AA, Butler MP, Brown SM, & Dubin AE (2003). Neuronal Hyperpolarization-Activated Pacemaker Channels Drive Neuropathic Pain. *Journal of Neuroscience* **23**, 1169–1178.

Chen X, Pang RP, Shen KF, Zimmermann M, Xin WJ, Li YY & Liu XG (2011). TNF-α enhances the currents of voltage gated sodium channels in uninjured dorsal root ganglion neurons following motor nerve injury. *Exp Neurol* **227**, 279–286.

Copray JC, Mantingh I, Brouwer N, Biber K, Kust BM, Liem RS, Huitinga I, Tilders FJ, VanDam AM, & Boddeke HW (2001). Expression of interleukin-1 beta in rat dorsal root ganglia. *J Neuroimmunol* **118**, 203–211.

Costigan M, Scholz J & Woolf CJ (2009). Neuropathic pain: a maladaptive response of the nervous system to damage. *Annu Rev Neurosci* **32**, 1–32.

Czeschik JC, Hagenacker T, Schafers M & Busselberg D (2008). TNF-α differentially modulates ion channels of nociceptive neurons. *Neurosci Lett* **434**, 293–298.

Dableh LJ, Yashpal K & Henry JL (2011). Neuropathic pain as a process: reversal of chronification in an animal model. *J Pain Res* **4**, 315–323.

Devor M, Vaso A, Adahan HM & Vyshka G (2014). PNS origin of phantom limb sensation and pain: Reply to Letter to the Editor regarding Foell et al., Peripheral origin of phantom limb pain: Is it all resolved? *Pain* **155**, 2207–2208.

Dib-Hajj SD, Black JA, Cummins TR, Kenney AM, Kocsis JD & Waxman SG (1998). Rescue of α-SNS sodium channel expression in small dorsal root ganglion neurons after axotomy by nerve growth factor in vivo. *J Neurophysiol* **79**, 2668–2676.

DiFrancesco D & Tortora P (1991). Direct activation of cardiac pacemaker channels by intracellular cyclic AMP. *Nature* **351**, 145–147.

Dobierzewska A, Shi L, Karakashian AA, & Nikolova-Karakashian MN (2012). Interleukin 1beta regulation of FoxO1 protein content and localization: evidence for a novel ceramide-dependent mechanism. *J Biol Chem* **287**, 44749–44760.

Emery EC, Young GT, Berrocoso EM, Chen L, & McNaughton PA (2011). HCN2 ion channels play a central role in inflammatory and neuropathic pain. *Science* **333**, 1462–1466.

Everill B & Kocsis JD (1999). Reduction of potassium currents in identified cutaneous afferent dorsal root ganglion neurons after axotomy. *J Neurophysiol* **82**, 700–708.

Everill B & Kocsis JD (2000). Nerve growth factor maintains potassium conductance after nerve injury in adult cutaneous afferent dorsal root ganglion neurons. *Neuroscience* **100**, 417–422.

Fitzgerald EM (2002). The presence of Ca2+ channel beta subunit is required for mitogen-activated protein kinase (MAPK)-dependent modulation of alpha1B Ca2+ channels in COS-7 cells. *J Physiol* **543**, 425–437.

Funakoshi M, Sonoda Y, Tago K, Tominaga S, & Kasahara T (2001). Differential involvement of p38 mitogen-activated protein kinase and phosphatidyl inositol 3-kinase in the IL-1-mediated NF-kappa B and AP-1 activation. *Int Immunopharmacol* **1**, 595–604.

Gabay E, Wolf G, Shavit Y, Yirmiya R & Tal M (2011). Chronic blockade of interleukin-1 (IL-1) prevents and attenuates neuropathic pain behavior and spontaneous ectopic neuronal activity following nerve injury. *Eur J Pain* **15**, 242–248.

Gilron I, Watson CP, Cahill CM & Moulin DE (2006). Neuropathic pain: a practical guide for the clinician. *CMAJ* **175**, 265–275.

Gold MS, Shuster MJ & Levine JD (1996). Characterization of six voltage-gated K^+ currents in adult rat sensory neurons. *J Neurophysiol* **75**, 2629–2646.

Govrin-Lippmann R & Devor M (1978). Ongoing activity in severed nerves: source and variation with time. *Brain Res* **159**, 406–410.

Gray T, Nettesheim P, Loftin C, Koo JS, Bonner J, Peddada S, & Langenbach R (2004). Interleukin-1beta-induced mucin production in human airway epithelium is mediated by cyclooxygenase-2, prostaglandin E2 receptors, and cyclic AMP-protein kinase A signaling. *Mol Pharmacol* **66**, 337–346.

Hagiwara K, Nunoki K, Ishii K, Abe T, & Yanagisawa T (2003). Differential inhibition of transient outward currents of Kv1.4 and Kv4.3 by endothelin. *Biochem Biophys Res Commun* **310**, 634–640.

Harper AA & Lawson SN (1985). Conduction velocity is related to morphological cell type in rat dorsal root ganglion neurones. *J Physiol* **359**, 31–46.

Kajander JC & Bennett GJ (1992). Onset of a painful peripheral neuropathy in rat: a partial and differential deafferentation and spontaneous discharge in Aβ and Aδ primary afferent neurons. *J Neurophysiol* **68**, 734–744.

Kaplan DR & Stephens RM (1994). Neurotrophin signal transduction by the Trk receptor. *J Neurobiol* **25**, 1404–1407.

Kim DS, Choi JO, Rim HD & Cho HJ (2002). Downregulation of voltage-gated potassium channel α gene expression in dorsal root ganglia following chronic constriction injury of the rat sciatic nerve. *Brain Res Mol Brain Res* **105**, 146–152.

Kouranova EV, Strassle BW, Ring RH, Bowlby MR, & Vasilyev DV (2008). Hyperpolarization-activated cyclic nucleotide-gated channel mRNA and protein expression in large versus small diameter dorsal root ganglion neurons: correlation with hyperpolarization-activated current gating. *Neuroscience* **153**, 1008–1019.

Kim KJ, Yoon YW & Chung JM (1997). Comparison of three rodent models of neuropathic pain. *Exp Brain Res* **113**, 200–206.

Kroner A, Greenhalgh AD, Zarruk JG, Passos Dos Santos R, Gaestel M & David S (2014). TNF and increased intracellular iron alter macrophage polarization to a detrimental M1 phenotype in the injured spinal cord. *Neuron* **83**, 1098–1116.

Lawson SN (2002). Phenotype and function of somatic primary afferent nociceptive neurones with C-, Aδ- or Aα/β-fibres. *Exp Physiol* **87**, 239–244.

Leung L & Cahill CM (2010). TNF-α and neuropathic pain–a review. *J Neuroinflammation* **7**, 27.

Li J & Baccei ML (2011). Pacemaker neurons within newborn spinal pain circuits. *J Neurosci* **31**, 9010–9022.

Lindsay RM (1988). Nerve growth factors (NGF, BDNF) enhance axonal regeneration but are not required for survival of adult sensory neurons. *J Neurosci* **8**, 2394–2405.

Liu L, Yang TM, Liedtke W, & Simon SA (2006). Chronic IL-1beta Signaling Potentiates Voltage-Dependent Sodium Currents in Trigeminal Nociceptive Neurons. *J Neurophysiol* **95**, 1478–1490.

Lu KT, Wang YW, Wo YY, & Yang YL (2005). Extracellular signal-regulated kinase-mediated IL-1-induced cortical neuron damage during traumatic brain injury. *Neurosci Lett* **386**, 40–45.

Ma C, Shu Y, Zheng Z, Chen Y, Yao H, Greenquist KW, White FA & LaMotte RH (2003). Similar electrophysiological changes in axotomized and neighboring intact dorsal root ganglion neurons. *J Neurophysiol* **89**, 1588–1602.

MacGillivray MK, Cruz TF, & McCulloch CA (2000). The recruitment of the interleukin-1 (IL-1) receptor-associated kinase (IRAK) into focal adhesion complexes is required for IL-1beta -induced ERK activation. *J Biol Chem* **275**, 23509–23515.

Maier JA, Hla T, & Maciag T (1990). Cyclooxygenase is an immediate-early gene induced by interleukin-1 in human endothelial cells. *J Biol Chem* **265**, 10805–10808.

Mika J, Korostynski M, Kaminska D, Wawrzczak-Bargiela A, Osikowicz M, Makuch W, Przewlocki R, & Przewlocka B (2008). Interleukin-1 alpha has antiallodynic and antihyperalgesic activities in a rat neuropathic pain model. *Pain* **138**, 587–597.

Mayer ML & Westbrook GL (1983). A voltage-clamp analysis of inward (anomalous) rectification in mouse spinal sensory ganglion neurones. *J Physiol* **340**, 19–45.

Mosconi T & Kruger L (1996). Fixed-diameter polyethylene cuffs applied to the rat sciatic nerve induce a painful neuropathy: ultrastructural morphometric analysis of axonal alterations. *Pain* **64**, 37–57.

Nadeau S, Filali M, Zhang J, Kerr BJ, Rivest S, Soulet D, Iwakura Y, deRivero Vaccari JP, Keane RW & Lacroix S (2011). Functional recovery after peripheral nerve injury is dependent on the pro-inflammatory cytokines IL-1β and TNF: implications for neuropathic pain. *J Neurosci* **31**, 12533–12542.

Obreja O, Rathee PK, Lips KS, Distler C, & Kress M (2002). IL-1 beta potentiates heat-activated currents in rat sensory neurons: involvement of IL-1RI, tyrosine kinase, and protein kinase C. *FASEB J* **16**, 1497–1503.

Nitzan-Luques A, Devor M & Tal M (2011). Genotype-selective phenotypic switch in primary afferent neurons contributes to neuropathic pain. *Pain* **152**, 2413–2426.

Pitcher GM & Henry JL (2008). Governing role of primary afferent drive in increased excitation of spinal nociceptive neurons in a model of sciatic neuropathy. *Exp Neurol* **214**, 219–228.

Sarantopoulos CD, McCallum JB, Rigaud M, Fuchs A, Kwok WM, & Hogan QH (2007). Opposing effects of spinal nerve ligation on calcium-activated potassium currents in axotomized and adjacent mammalian primary afferent neurons. *Brain Res* **1132**, 84–99.

Scholz J & Woolf CJ (2007). The neuropathic pain triad: neurons, immune cells and glia. *Nat Neurosci* **10**, 1361–1368.

Scroggs RS, Todorovic SM, Anderson EG, & Fox AP (1994). Variation in IH, IIR, and ILEAK between acutely isolated adult rat dorsal root ganglion neurons of different size. *J Neurophysiol* **71**, 271–279.

Shipston MJ, Duncan RR, Clark AG, Antoni FA, & Tian L (1999). Molecular components of large conductance calcium-activated potassium (BK) channels in mouse pituitary corticotropes. *Mol Endocrinol* **13**, 1728–1737.

Sommer C & Kress M (2004). Recent findings on how proinflammatory cytokines cause pain: peripheral mechanisms in inflammatory and neuropathic hyperalgesia. *Neurosci Lett* **361**, 184–187.

Stamboulian S, Choi JS, Ahn HS, Chang YW, Tyrrell L, Black JA, Waxman SG, & Dib-Hajj SD (2010). ERK1/2 mitogen-activated protein kinase phosphorylates sodium channel Na(v)1.7 and alters its gating properties. *J Neurosci* **30**, 1637–1647.

Stemkowski PL & Smith PA (2010). Long-term interleukin-1β exposure increases small IB4-positive and medium sensory neuron excitability by differential actions on ionic conductances. Program No. 175.2. *2010 Neuroscience Meeting Planner. Society for Neuroscience, Washington, DC.*

Stemkowski PL, Jones KE & Smith PA (2011). Long-term interleukin-1β exposure increases small IB4-positive and medium sensory neuron excitability by differential actions on ionic conductances. *Program and Abstracts from the Fifth Annual Canadian Neuroscience Meeting*, 102–103.

Stemkowski PL & Smith PA (2012*a*). Long-term IL-1beta exposure causes subpopulation-dependent alterations in rat dorsal root ganglion neuron excitability. *J Neurophysiol* **107**, 1586–1597.

Stemkowski PL & Smith PA (2012*b*). Sensory neurons, ion channels, inflammation and the onset of neuropathic pain. *Can J Neurol Sci* **39**, 416–435.

Sukhotinsky I, Ben Dor E, Raber P & Devor M (2004). Key role of the dorsal root ganglion in neuropathic tactile hypersensibility. *Eur J Pain* **8**, 135–143.

Tan ZY, Donnelly DF & LaMotte RH (2006). Effects of a chronic compression of the dorsal root ganglion on voltage-gated Na^+ and K^+ currents in cutaneous afferent neurons. *J Neurophysiol* **95**, 1115–1123.

Treede R-D, Jensen TS, Campbell JN, Cruccu G, Dostrovsky JO, Griffin JW, Hansson P, Hughes R, Nurmikko T & Serra J (2008). Neuropathic pain: Redefinition and a grading system for clinical and research purposes. *Neurology* **70**, 1630–1635.

Vaso A, Adahan HM, Gjika A, Zahaj S, Zhurda T, Vyshka G & Devor M (2014). Peripheral nervous system origin of phantom limb pain. *Pain* **155**, 1384–1391.

Wainger BJ, DeGennaro M, Santoro B, Siegelbaum SA, & Tibbs GR (2001). Molecular mechanism of cAMP modulation of HCN pacemaker channels. *Nature* **411**, 805–810.

Wall PD, Devor M, Inbal R, Scadding JW, Schonfeld D, Seltzer Z & Tomkiewicz MM (1979). Autotomy following peripheral nerve lesions: experimental anaesthesia dolorosa. *Pain* **7**, 103–113.

Watkins LR & Maier SF (1999). Implications of immune-to-brain communication for sickness and pain. *Proc Natl Acad Sci U S A* **96**, 7710–7713.

Watkins LR & Maier SF (2002). Beyond neurons: Evidence that immune and glial cells contribute to pathological pain states. *Physiol Rev* **82**, 981–1011.

Waxman SG, Dib-Hajj S, Cummins TR & Black JA (1999). Sodium channels and pain. *Proc Natl Acad Sci U S A* **96**, 7635–7639.

Waxman SG & Zamponi GW (2014). Regulating excitability of peripheral afferents: emerging ion channel targets. *Nat Neurosci* **17**, 153–163.

Widmer HA, Rowe IC, & Shipston MJ (2003). Conditional protein phosphorylation regulates BK channel activity in rat cerebellar Purkinje neurons. *J Physiol* **552**, 379–391.

Wolf G, Gabay E, Tal M, Yirmiya R & Shavit Y (2006). Genetic impairment of interleukin-1 signaling attenuates neuropathic pain, autotomy, and spontaneous ectopic neuronal activity, following nerve injury in mice. *Pain* **120**, 315–324.

Yang KY, Bae WS, Kim MJ, Bae YC, Kim YJ, Kim HJ, Nam SH & Ahn DK (2013). Participation of the central p38 and ERK1/2 pathways in IL-1β-induced sensitization of nociception in rats. *Prog Neuropsychopharmacol Biol Psychiatry* **46**, 98–104.

Yao H, Donnelly DF, Ma C & LaMotte RH (2003). Upregulation of the hyperpolarization-activated cation current after chronic compression of the dorsal root ganglion. *J Neurosci* **23**, 2069–2074.

Additional information

Competing interests

None.

Author contributions

P.L.S. carried out the majority of the experiments and data analysis, and prepared the first draft of the manuscript. Additional experimental data were acquired and analysed by M-C. N. and Y.C. P.A.S. designed the study, supervised the experiments and edited the final version of the manuscript.

Funding

This work was supported by the Canadian Institutes of Health Research HOP126788. P.L.S. was supported by an Alberta Heritage Foundation for Medical Research (AHFMR) studentship and an AHFMR Dr Lionel E. McLeod Health Research Scholarship. M-C.N. was supported by an Alberta Innovates Health Sciences graduate student award.

Acknowledgements

We thank Miss Briana Napier and Dr Nataliya Bukhanova for help with data analysis.